

A critical step in the folding of influenza virus HA determined with a novel folding assay

M Claudia Maggioni^{1,2}, I Marije Liscaljet^{1,2} & Ineke Braakman¹

Most principles of protein folding emerged from refolding studies *in vitro* on small, soluble proteins, because large ones tend to misfold and aggregate. We developed a folding assay allowing the study of large proteins in detergent such that the extent of cellular assistance required for proper folding can be determined. We identified a critical step in the *in vivo* folding pathway of influenza virus hemagglutinin (HA). Only the formation of the first few disulfides in the top domain of HA required the intact endoplasmic reticulum. After that, HA proceeded to fold efficiently in a very dilute solution, despite its size and complexity. This study paves the way for detailed structural analyses during the folding of complex proteins.

Protein folding is the process by which linear polypeptide chains acquire their biologically active three-dimensional conformation. Although all information needed to reach the native conformation is encoded by the amino acid sequence¹, protein folding inside the cell generally is assisted by molecular chaperones and folding enzymes^{2–4}. They mainly protect nascent chains and newly synthesized proteins from misfolding and aggregation. Chaperones and folding enzymes reside in almost every compartment of eukaryotic cells.

The endoplasmic reticulum (ER) is highly specialized for the folding of membrane and secretory proteins. One of the best-characterized model proteins used to study protein folding in the ER is the influenza virus HA. This protein is not only crucial for influenza virus infection but also an important target for the immune system. HA is a multidomain glycoprotein of 84 kDa with six disulfide bonds and seven N-linked glycans. It folds in the ER, trimerizes and is transported to the plasma membrane, where it is incorporated into new virions. The folding of HA has been studied extensively both in complete cells^{5–11} and in microsomes^{12,13}, using radioactive labeling of newly synthesized HA or truncated ribosome-bound nascent chains¹⁴. Although these studies yielded fairly detailed information on the HA folding process, further molecular insight would require biophysical studies on purified protein, which would disregard the role of the cell.

To start bridging the gap between folding studies *in vitro* and in intact cells, we developed an assay that allows the study of post-translational HA folding in a cell-free system without membranes. We replaced the chase period in the well-established pulse-chase folding assay⁶ with a folding analysis in solution: the protein is translated and translocated in intact cells, after which post-translational folding is studied in a detergent cell lysate. Using this '*in vitro* chase' assay, we found that HA can fold in a detergent cell lysate without ER assistance, provided that the first folding step occurs in an intact ER.

RESULTS

HA can fold in a detergent cell lysate

When studied with the pulse-chase assay in intact cells, newly synthesized HA ran as a single band in a reducing SDS-PAGE gel (Fig. 1a, R) and as three bands in a nonreducing gel: the native, fully oxidized HA (NT) and two folding intermediates, IT1 and IT2 (Fig. 1a, NR)⁶. The two folding intermediates have lower electrophoretic mobility than NT because they still lack some of the six disulfide bonds, which render them less compact upon denaturation than NT. Even though the first two disulfide bonds always form during translation¹⁴, most of HA's folding occurs post-translationally^{6,10}.

For the *in vitro*-chase assay, influenza-infected cells were pulse-labeled for 2 min as in the pulse-chase assay, to translate HA *in vivo*. Cells were lysed immediately in a detergent-containing buffer and kept on ice. The nuclei were removed by centrifugation and the supernatant was transferred to an eppendorf tube. The diluted cell lysate contained detergent micelles instead of intact membranes, including radiolabeled folding intermediates of glycosylated full-length HA from which the signal peptide had been cleaved. We then started the oxidative *in vitro* folding process of HA by increasing the temperature and adding oxidized glutathione (GSSG). After various times of incubation, the *in vitro* chase was stopped as a conventional chase by cooling the sample on ice and alkylating the remaining free cysteines with *N*-ethylmaleimide (NEM) to block further disulfide bond formation.

HA folding in this very dilute system (Fig. 1b) was very similar to folding in intact cells (Fig. 1a): HA folded to NT and aggregates were undetectable; even the rate of folding was similar. The process was very efficient: we saw an increase from 27% NT to 70% NT during the *in vivo* chase (Fig. 1a) and an increase from 30% NT to 58% NT during the *in vitro* chase (Fig. 1b). The percent of NT was quantified as the ratio of the amount of NT to the total amount of HA in every lane (NT/total HA). We discounted aggregates because the fraction

¹Department of Cellular Protein Chemistry, Bijvoet Center for Biomolecular Research, Faculty of Chemistry, Utrecht University, Padualaan 8, 3584 CH Utrecht, The Netherlands. ²These authors contributed equally to this work. Correspondence should be addressed to I.B. (i.braakman@chem.uu.nl).

Published online 6 February 2005; doi:10.1038/nsmb897

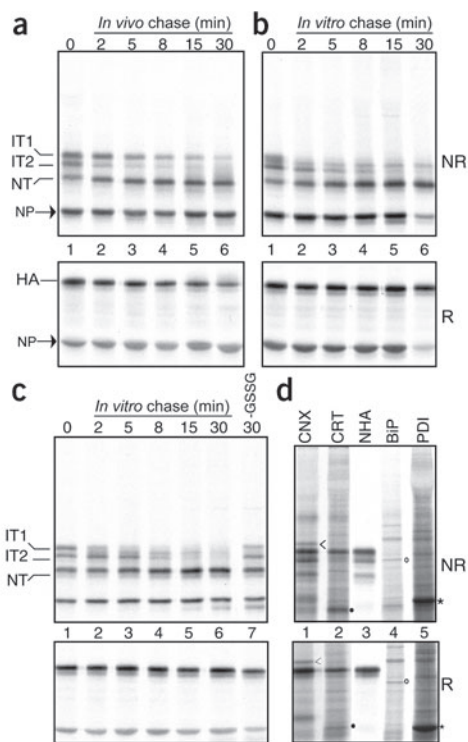


Figure 1 HA folds in a diluted detergent cell lysate. Fluorographs of ^{35}S -labeled HA analyzed by 7.5% (w/v) SDS-PAGE, nonreducing (NR) (top panels) or reducing (R) (bottom panels). **(a)** HA folding assay in intact CHO cells, monitored by pulse-chase (see Methods). Samples were immunoprecipitated using a polyclonal antiserum (P) against influenza virus recognizing all forms of HA and the influenza virus nucleoprotein (NP) (see Methods). The two HA folding intermediates (IT1 and IT2), native HA (NT), and influenza virus nucleoprotein (NP) are indicated. **(b)** HA folding was analyzed *in vitro*: influenza virus-infected cells were pulse-labeled for 2 min and lysed in ice-cold detergent containing buffer. To start the *in vitro* chase assay, the temperature was raised to 30 °C and 5 mM GSSG was added (see Methods). **(c)** Experiment was done as in **b** except that 1 mM DTT was present in the lysis buffer. In lane 7 the lysate was kept on ice without GSSG addition. **(d)** Antibodies against calnexin (CNX), calreticulin (CRT), HA (NHA), BiP and protein disulfide isomerase (PDI) were used for immunoprecipitations of a 0-min *in vitro*-chased sample. Cells were lysed either in 2% (w/v) CHAPS lysis buffer (lanes 1 and 2) or in 0.5% (v/v) Triton X-100 (lanes 3–5). See Methods. Immunoprecipitated chaperones are indicated: CNX (arrowhead), CRT (filled circle), BiP (open circle) and PDI (asterisk).

was low and did not change during the assay in CHO cells. Despite the overall similarity between the two folding assays, small differences could be seen: IT1 was not a sharp band at the beginning of the *in vitro* assay (Fig. 1b, lane 1), because the free cysteines in the sample were not immediately blocked by NEM in order to allow oxidative folding of the protein during the *in vitro* chase period. We have previously shown that IT1 is not stable in a cell lysate⁶. We experimentally determined that addition of 1 mM DTT to the lysis buffer was sufficient to keep IT1 as a sharp band without affecting the folding process of HA (Fig. 1c, lanes 1–6). Under these conditions, folding intermediates now were stable for at least 30 min if kept on ice in the absence of glutathione (Fig. 1c, lane 7). The downward shift of the NT band from lane 1 to lane 2 in Figure 1a, representing glucose (and perhaps already some mannose) trimming, was not present *in vitro* (Fig. 1c, lanes 1 and 2). The slight decrease in sharpness of HA folded *in vivo* at later time points (Fig. 1a, lanes 4–6), caused by complex glycosylation in the Golgi, was absent *in vitro* as well, as expected. Another difference with folding in intact cells was the appearance of a band between IT1 and IT2 *in vitro* (Fig. 1b, lanes 2–6). Its persistence suggests it to be an off-pathway form not leading to NT. This band is probably not the result of carbohydrate trimming because it appears only in nonreducing gels of the *in vitro* chase assay and in some cysteine

mutants (A. Azuaga-Fortes, Utrecht University, and I.B., unpublished observations).

The cell lysate contained all factors present in the intact cell but in highly diluted form. To characterize our *in vitro* chase lysate and to demonstrate whether dilution and the presence of detergent interfered with the binding of chaperones and folding factors, we used antibodies against molecular chaperones known to bind HA in intact cells^{15–17}. At the start of the *in vitro* chase assay, HA was found in a complex with calnexin (CNX) and calreticulin (CRT), but we did not detect association with ERp57 (data not shown), BiP or PDI (Fig. 1d).

HA folded *in vitro* acquires correct epitopes

To confirm conformational and antigenic resemblance between HA folded in the intact cell versus HA folded in the cell lysate, we used a series of conformation-specific antibodies (Fig. 2). As shown in the schematic structure of HA (Fig. 2a), F1 and F2 are monoclonal antibodies against epitopes in the stem domain that recognize early and late folding intermediates, respectively^{6,7}. *In vivo*, F1 recognizes only the relatively unfolded forms of HA: it precipitates reduced HA, folding intermediate IT1 and folding intermediate IT2, but not the native

Figure 2 *In vitro* folded HA acquires the correct epitopes. **(a)** Schematic diagram of the three-dimensional structure of monomeric HA (X31) as it is present in the trimer, at neutral pH (based on a reported crystal structure²³), consisting of a top globular domain composed mainly of β -sheets and a stem domain composed of α -helices. Conformational epitopes are indicated as A, B, E, F1 and F2. The blue box presents the 12 cysteines (yellow circles) involved in disulfide bonds and the orange box presents the position of the 7 N-linked glycans (red triangles: 5 visible, 2 behind the strands). **(b)** *In vitro*-chased samples were generated as in Figure 1c, with a 2-min *in vivo* pulse and a 30-min *in vitro* chase. Conformational antibodies against the top domain epitopes A, B and E, and antibodies F1 and F2 against the stem domain were used for immunoprecipitation.

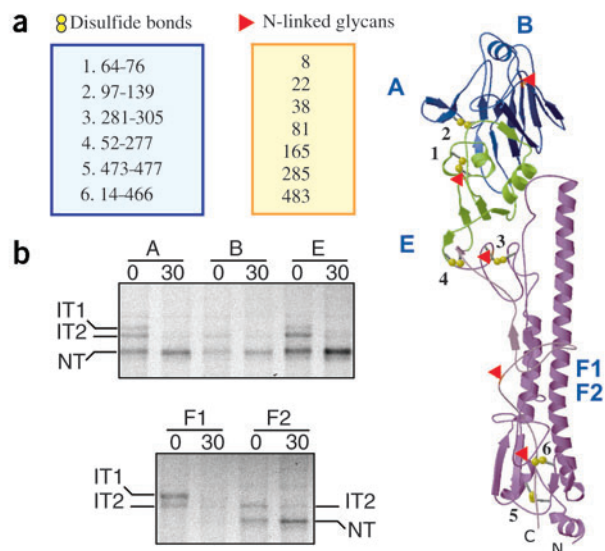
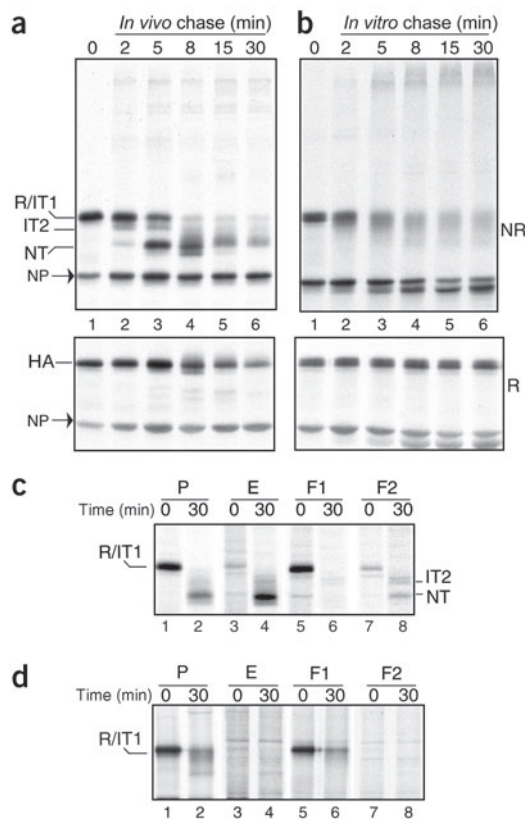


Figure 3 Reduced HA cannot fold in a diluted lysate. Samples were prepared and analyzed as in **Figure 1a,b**, except that 5 mM DTT was added during the 5-min pulse-labeling to prevent disulfide bond formation during synthesis. **(a,b)** As a consequence, oxidative folding could start only during the chase in intact cells **(a)**, but not during the *in vitro* chase **(b)**. **(c,d)** Analysis of conformation-specific antibodies of early and late chase time points from *in vivo* **(c)** or *in vitro* **(d)** chase samples. Different exposure times were used for the immunoprecipitation with P versus conformational antibodies. Reduced HA and folding intermediate IT1 cannot be resolved on this gel (R/IT1).



NT form^{6,7}. In contrast, F2 precipitates IT2 and early NT, but not IT1 or mature trimeric HA^{6,10,18}. The monoclonal antibodies HC3, HC19 and HC100 recognize epitopes A, B and E in the top domain (**Fig. 2a**), which are formed in some HA chains already during synthesis and in others immediately after synthesis¹⁸, indicating heterogeneity in the folding process. These epitopes persist throughout HA's lifetime¹⁸. We concluded from the immunoprecipitations of *in vitro*-chased samples with the five antibodies (**Fig. 2b**) that each antibody reacted with the different forms of HA as expected^{6,10,18}: the A, B, and E epitopes were present both early (0 min) and late (30 min), whereas the F1 antibody recognized little HA after a 30-min *in vitro* chase. F2 did not detect IT1 and immunoprecipitated IT2 and NT, but instead of a decrease in recognition with time, it interacted strongly with NT at 30 min. *In vivo*, F2 loses its epitope around the time of HA trimerization, and HA is not likely to trimerize in this diluted system in the absence of membranes^{18,19}. Indeed, HA trimers were not detectable after folding in the lysate: HA did not precipitate with the trimer-specific antibody N2, and did not reach trypsin resistance as it does *in vivo*²⁰ (data not shown). Taken together, the results show that in a cell lysate in the absence of an intact ER, HA monomers folded into their proper, native conformation with high efficiency.

Reduced HA cannot fold in a cell lysate

We demonstrated that HA folds properly in a detergent cell lysate, even though this protein is large and complex. On the other hand, the starting point of the folding assay was not an unfolded protein, but rather an HA molecule partially folded during translation. To study whether the detergent cell lysate would also support the earlier steps of folding, we prevented oxidative folding *in vivo* by pulse-labeling HA in the presence of DTT (**Fig. 3**). In intact cells, disulfide bond formation can be postponed successfully until synthesis is completed: HA starts to form its disulfide bonds as soon as DTT is removed (**Fig. 3a**, lane 2), with little adverse effect on the outcome of folding^{7,21} as confirmed by analysis with conformation-specific antibodies (**Fig. 3c**).

During the *in vitro* chase assay, the reduced and largely unfolded HA oxidized in the lysate upon addition of GSSG, but distinct folding intermediates did not appear (**Fig. 3b**). The fraction of HA that aggregated increased, and NT did not form. In some experiments (**Fig. 3d**, lane 2, and **Fig. 5a**, lane 6), oxidation went as far as an NT-like form, but analysis with conformation-specific antibodies confirmed that none of the top domain epitopes were ever formed (**Figs. 3d** (only the E epitope is shown) and **5b**). In addition, F2 did not recognize any of the oxidized forms, whereas F1 still recognized some reduced HA after the *in vitro* chase. We concluded that HA could not fold from a completely reduced state in the absence of an intact ER; it needed to acquire some disulfide bonds *in vivo* first.

The presence of DTT during HA synthesis prevented the formation of disulfide bonds as well as the acquisition of some conformation⁷ that could be crucial for productive folding in the cell lysate. We tested whether post-translational reduction of partially oxidized HA would allow folding in the cell lysate, which would suggest maintenance of critical conformation acquired during synthesis, despite reduction of the already formed disulfide bonds. In other words, we analyzed whether the history of the reduced HA molecule or its state at the start of the *in vitro* folding phase determined its competence for folding. The results showed that, irrespective of whether HA had formed disulfide bonds during synthesis, the reduced protein could not fold in the lysate (data not shown).

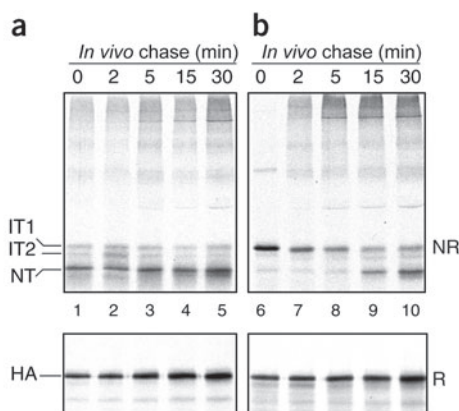
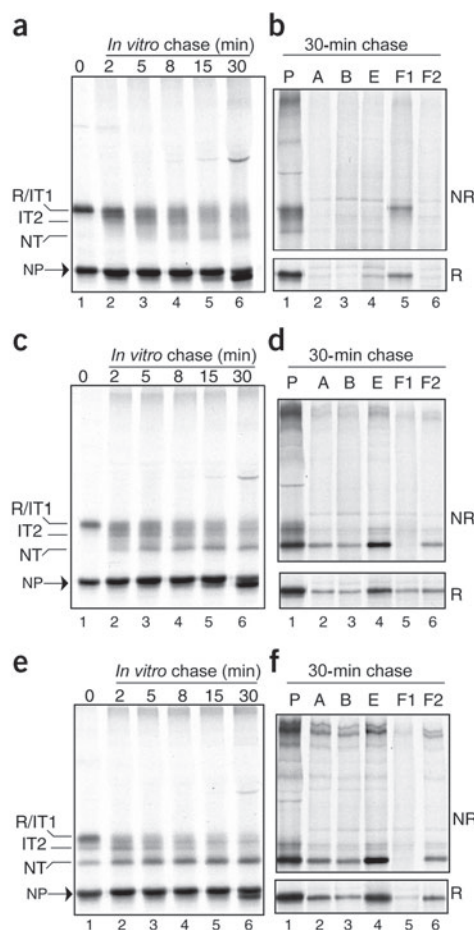


Figure 4 Reduced HA can fold *in vivo* in the absence of CNX or CRT binding. **(a,b)** Lec23 cells expressing HA via recombinant Vaccinia virus infection and transfection were analyzed as in **Figure 1a** **(a)** or were preincubated for 5 min and pulse-labeled in the presence of 5 mM DTT **(b)**. Cells then were chased in the absence of DTT for the indicated times, lysed and analyzed as in **Figure 1**.

Figure 5 The bottleneck of HA folding: formation of the first few disulfides. Samples were prepared and analyzed as in **Figure 3b**. (**a–f**) Nonreducing gels (**a, c** and **e**) and both nonreducing and reducing gels (**b, d** and **f**) are shown. The starting point of the *in vitro* chase was either completely reduced HA from a pulse in DTT (**a**, as in **Fig. 3b**), or HA pulse-labeled in the presence of DTT, but rescued in a chase in intact cells without DTT for 1 min (**c**) or 5 min (**e**). Analysis of a 30 min *in vitro* chase sample, rescued for 0 (**b**), 1 (**d**) or 5 (**f**) min *in vivo*, with conformation-specific antibodies. Different exposure times were used for the immunoprecipitation with P versus the conformational antibodies.



Reduced HA folds *in vivo* without CNX or CRT

Whereas partially folded HA did fold in the absence of an intact ER, completely reduced HA did not (**Figs. 3b** and **5a**). Because CNX binding to HA is inhibited by the presence of DTT¹⁶ we needed to check whether lack of CNX rebinding *in vitro* caused improper oxidation of HA *in vitro*. To exclude a role for CNX, we used CHO-derived Lec23 cells, which lack glucosidase I activity and therefore do not support CNX or CRT association with substrate proteins in the ER²². We reasoned that proper folding from reduced HA should not be possible in the Lec23 cells if CNX or CRT were essential for this step. We therefore compared folding of HA in intact Lec23 cells (**Fig. 4**) without DTT (as in **Fig. 1a**) and with DTT (as in **Fig. 3a**) in the pulse medium. Because HA needs CNX for folding¹¹, a relatively large fraction of HA aggregated in the control experiment without DTT (**Fig. 4a**). When HA was synthesized in the presence of DTT (**Fig. 4b**), the portion that aggregated was similar to that in **Figure 4a**, but the rest of HA folded to NT in the cell (**Fig. 4b**, lanes 4 and 5) and trimerized (data not shown). We concluded that, even in the absence of CNX binding, HA can fold from the reduced form *in vivo*. Clearly, in the *in vitro* assay, HA itself could not nucleate proper folding from the reduced state.

The critical step during HA folding

To determine the minimal conformation that needed to form in the intact ER for productive folding in solution, we pulse-labeled HA in the presence of DTT, followed by short *in vivo* 'rescue chases' without DTT (**Fig. 5**). With increasing times of rescue chase, from 0 to 1 or 5 min (**Fig. 5a,c,e**, lane 1), HA acquired an increasing number of disulfide bonds and native epitopes in the intact ER, before lysis of the cells and the start of the *in vitro* folding phase. The longer the *in vivo* rescue time, the more NT had formed after 30 min of *in vitro* chase (compare lane 6 in **Fig. 5a,c,e**). Although HA was still mainly in the form of R/IT1 after only 1 min of rescue (**Fig. 5c**, lane 1), a large fraction of HA could fold to NT in the lysate (**Fig. 5c**, lane 6). We concluded that formation of IT2 was not a prerequisite to reach the NT form *in vitro*. Analysis of the 30-min *in vitro* chase samples with the conformation-specific antibodies (**Fig. 5b,d,f**) confirmed that, whereas neither the top domain epitopes nor F2 were present immediately after the pulse (**Fig. 5b**), all the top domain epitopes as well as the

F2 epitope had formed already when a 1-min rescue in intact cells was allowed before the *in vitro* chase (**Fig. 5d**). In agreement with this, the F1 epitope disappeared (compare lane 5 in **Fig. 5d,f** and **Fig. 5b**). We concluded that formation of the first two disulfides (IT1), or perhaps even only the first one, was sufficient to allow productive HA folding during the *in vitro* chase.

To confirm that rebinding of CNX during the *in vivo* chase was not the reason for the rescue of HA folding *in vitro*, we repeated the experiment shown in **Figure 5** in Lec23 cells (**Fig. 6**). Aside from the aggregates and the slower folding from reduced HA in Lec23 cells, the results were similar to those for the CHO cells, showing that the absence or presence of CNX binding is not the source of the difference in folding competence of reduced HA versus IT1. Combining our results from the Lec23 cells, we conclude that CNX and CRT are not needed for passing the bottleneck *in vivo*, and do not play an essential role in the subsequent folding of HA to NT *in vitro*.

A previous study showed that disulfide 1 (64-76) in the top domain of HA can already form on the nascent chain¹⁴. Because IT2 corresponds to the closure of disulfide 4 (52-277) and NT corresponds to closure of disulfide 6 (14-466)¹⁰ (I.B. *et al.*, unpublished data), our results suggest that only the first few small disulfide bonds need to form *in vivo* to allow further folding of HA in the detergent lysate. Combining all our results,

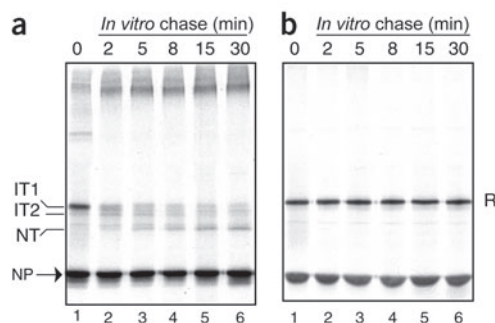


Figure 6 Rescue of reduced HA in the absence of calnexin binding. The experiment was done exactly as in **Figure 5**, but in Lec23 cells. (**a,b**) *In vivo* rescue time was 5 min and samples were analyzed using nonreducing (**a**) and reducing (**b**) 7.5% (w/v) SDS-PAGE.

we conclude that, whereas the major part of HA folding works in a highly diluted cell lysate, an intact ER is required for the formation of the first small disulfide bond(s) in HA's top domain.

DISCUSSION

We established a new *in vitro* assay for the folding of large, complex proteins based on our 'pulse-chase' folding assay in intact cells. Using this assay, we identified a bottleneck in the folding of influenza virus HA: the protein folded properly and productively in a highly diluted detergent cell lysate provided its first small disulfides were formed in the intact ER. The HA molecules folded *in vitro* correctly in every determinable aspect.

HA is structured like a hairpin²³ that folds from the tip of the bend, the top domain, toward the N and C terminus of the ectodomain at the bottom of the stem¹⁰. Our results indicate that the critical step during HA folding is the formation of IT1, which *in vivo* occurs cotranslationally and involves the closure of the first two small disulfide loops in the top domain of HA, 1 (64-76) and 2 (97-139)^{10,14} (I.B. *et al.*, unpublished data). We indeed found that mutation of the disulfide bond 1 (64-76) in the top domain completely blocked folding of HA beyond R/IT1. It is no surprise to us that the most critical of the seven glycans present in HA also resides in this area, at position 81 (ref. 16).

Although formation of IT1 always occurs cotranslationally^{10,14}, this step can be postponed until after synthesis in the intact cell^{7,10}. From these and other *in vivo* data we had concluded before that the termination of translation does not correlate with a specific folding step in HA, but that certain folding steps occur sometimes during and sometimes after synthesis. We have now identified an early step in HA folding that has three characteristics: it is the most critical, it is always cotranslational^{6,7,10}, and it can occur post-translationally *in vivo* but not *in vitro*. This may not be a coincidence. Perhaps sequential folding of the HA nascent chain during translation and/or protection by the ribosome-translocon complex²⁴ does contribute to the passage of this critical step.

If it does not happen on the nascent chain, formation of IT1 clearly needs assistance from chaperones and folding enzymes, assistance that is lacking in our *in vitro* chase assay. CNX and CRT were still found associated with HA *in vitro*, but although these and other chaperones and folding enzymes are still present in the detergent lysate, they were diluted so much that they are unlikely to exhibit their physiological activity, especially when cochaperones are involved²⁵. We were thus not surprised that we found no essential role for CNX and CRT during *in vitro* folding. Our assay distinguished the early, critical ER-dependent step from the later, ER-independent stages of HA folding: formation of the first disulfide(s) in the top domain region is required but also sufficient to allow further folding without extensive ER assistance in a detergent cell lysate. Considering the virtually complete conservation^{26,27} of the 12 cysteines in HA of all influenza strains, the identification of HA's Achilles' heel opens new avenues for the design of antiviral drugs.

An earlier attempt to study folding of a viral protein *in vitro* used the VSV-G protein purified from the mature virion: VSV-G folded with very low efficiency and ~50% aggregation²⁸. Other cell-free studies with complex proteins^{12,29} are based on microsomes; the possibility of modulating the folding environment is limited and protein synthesis and translocation seem less efficient than in living cells.

The assay we developed presents the advantages of both *in vivo* and *in vitro* studies: the protein of interest is synthesized in an intact cell, ensuring that post-translational modifications occur and that correct initial assistance is given; the option to modulate the '*in vivo*' phase in nature and length combined with the high dilution of the *in vitro* chase

allows the determination of how long cellular assistance is needed during the folding process and whether any ER-independent folding step exists. The lack of membranes in the second phase of the experiment allows easy manipulation of the folding milieu. It now has become possible to study complex, large, multidomain proteins in a highly diluted solution. With this assay, we constructed another segment of a bridge between *in vitro* and *in vivo* folding studies.

METHODS

Cell lines, viruses, and HA expression. Chinese hamster ovary cells (CHO) were cultured in α MEM (Gibco-BRL) and Lec23 cells²² in α MEM with nucleosides (Gibco-BRL) supplemented with 8% (v/v) FCS (Gibco-BRL), 100 U ml⁻¹ each of streptomycin and penicillin and 2 mM glutamax (Gibco-BRL).

The X31 strain of influenza virus, A/Aichi/1968/H3N2, was used for all infections. Cells were infected in RPMI medium, 0.2% (w/v) BSA, 10 mM HEPES, pH 6.8, and rocked at 37 °C in the absence of CO₂. After 1 h, complete culture medium was added to the dishes, which were then incubated at 37 °C in the presence of CO₂.

Recombinant vaccinia virus expressing T7 polymerase³⁰ was used for HA expression (Fig. 4). Subconfluent Lec23 cells were infected and transfected as described³¹ and incubated at 37 °C.

***In vivo* pulse-chase analysis of HA.** Subconfluent CHO cells (unless indicated otherwise) were pulse-labeled 5 h after infection with influenza or recombinant vaccinia virus⁶. Metabolic labeling was done as described⁶. Briefly, cells were starved for 15–30 min in cysteine- and methionine-free medium and then pulsed for 2 min with Revidu PRO-MIX L-[³⁵S] *in vitro* cell labeling mix (Amersham Biosciences). When indicated, a 5-min preincubation and a 5-min pulse were carried out in the presence of 5 mM DTT, followed or not by a chase for different times with an excess of unlabeled cysteine and methionine. Chase samples were stopped by aspirating the medium and adding ice-cold HBSS (Gibco-BRL) containing 20 mM NEM (Sigma) to block the free sulfhydryl groups. Cells were lysed in cold MNT (20 mM MES, 100 mM NaCl, 30 mM Tris-HCl, pH 7.5) containing 0.5% (v/v) Triton X-100, 10 μ g ml⁻¹ each of chymostatin, leupeptin, antipain and pepstatin and 1 mM PMSF. Cell lysates were spun for 10 min at 15,000g to pellet the nuclei and supernatants were used for immunoprecipitation.

***In vitro* chase assay.** CHO or Lec23 cells were pulse-labeled with or without 5 mM DTT in intact cells as described above. After the pulse (and sometimes a short chase), cells were washed twice with ice-cold HBSS (Gibco-BRL), immediately lysed with ice-cold MNT (20 mM MES, 100 mM NaCl, 30 mM Tris-HCl, pH 7.5) containing 0.5% (v/v) Triton X-100, 10 μ g ml⁻¹ each of chymostatin, leupeptin, antipain and pepstatin and 1 mM PMSF. After scraping of cells, 20 mM NEM was immediately added to 1/6 of the lysate (this is the 0-min sample of the *in vitro* assay). All cell lysates were then centrifuged for 10 min at 15,000g and 4 °C to pellet nuclei. The supernatant of the lysate without NEM was transferred to a new tube for the *in vitro* chase assay. To start the *in vitro* folding phase, 5 mM GSSG (Roche) was added and the tube was immediately transferred to a 30 °C waterbath. After different times of incubation, part of the lysate was transferred to a new tube on ice containing NEM to a final concentration of 20 mM to block free cysteines. Samples were kept on ice until being subjected to immunoprecipitation.

Immunoprecipitation and SDS-PAGE. Immunoprecipitations were carried out as described⁶ with a polyclonal rabbit antiserum against the N terminus of HA, when indicated (NHA), or with a polyclonal rabbit antiserum (P) against X-31 virus, which recognizes all forms of HA as well as the nucleoprotein (NP), which is a phosphoprotein^{32–34} and can appear as either one or two bands in the gel depending on the phosphorylation status of the protein (A. Ora, Utrecht University, and I.B., unpublished observations). To probe for different conformations, two mouse monoclonal IgG antibodies, F1 and F2, made against non-denatured HA2 were used⁶. The mouse monoclonal antibodies HC3, HC19 and HC100, mapped against epitopes A, B and E, respectively, all in the top domain of HA, have been described^{7,20,35,36}. For coimmunoprecipitation with known chaperones, cells were either lysed in 2% (w/v) CHAPS in HBS (50 mM HEPES, pH 7.6, 200 mM NaCl) or in 0.5% (v/v) Triton X-100 lysis buffer (as described above). Cell lysates were precleared with heat-killed and fixed *Staphylococcus*

aureus cells. Immunoprecipitates were washed in 0.5% (w/v) CHAPS in HBS or 0.5% (v/v) Triton X-100 lysis buffer. Coimmunoprecipitation of HA with CNX and CRT from a pulse-chase in intact cells was similar when carried out in Triton X-100 or in CHAPS lysis buffer (B. Kleizen, Utrecht University, and I.B., unpublished observation). The CNX antibody was provided by A. Helenius (ETH, Zürich). The polyclonal antibody against CRT was purchased from Affinity BioReagents. The BiP antibody was purchased from Stressgen, and the PDI antibody has been described³⁷. Immunoprecipitated HA was resolved on nonreducing and reducing 7.5% (w/v) SDS-PAGE.

ACKNOWLEDGMENTS

We thank H. Tabak, A. Ora and A. Azuaga-Fortes for comments, discussions and critical reading of the manuscript, and B. Kleizen, M. Molinari, A. Helenius and members of the Braakman lab for fruitful discussions. We thank J. Smit for preparing the cartoon of HA (Fig. 2a). The work was supported by a grant from Telethon Foundation, Italy (M.C.M.), a European Union Marie Curie Research Training grant (M.C.M.), and Netherlands Organization for Scientific Research/Chemical Sciences (I.M.L. and I.B.).

COMPETING INTERESTS STATEMENT

The authors declare that they have no competing financial interests.

Received 27 September 2004; accepted 4 January 2005

Published online at <http://www.nature.com/nsmb/>

- Anfinsen, C.B. Principles that govern the folding of protein chains. *Science* **181**, 223–230 (1973).
- Gething, M.J. & Sambrook, J. Protein folding in the cell. *Nature* **355**, 33–45 (1992).
- Hartl, F.U. Molecular chaperones in cellular protein folding. *Nature* **381**, 571–579 (1996).
- Kleizen, B. & Braakman, I. Protein folding and quality control in the endoplasmic reticulum. *Curr. Opin. Cell Biol.* **16**, 343–349 (2004).
- Copeland, C.S. *et al.* Folding, trimerization, and transport are sequential events in the biogenesis of influenza virus hemagglutinin. *Cell* **53**, 197–209 (1988).
- Braakman, I., Hoover-Litty, H., Wagner, K.R. & Helenius, A. Folding of influenza hemagglutinin in the endoplasmic reticulum. *J. Cell Biol.* **114**, 401–411 (1991).
- Braakman, I., Helenius, J. & Helenius, A. Manipulating disulfide bond formation and protein folding in the endoplasmic reticulum. *EMBO J.* **11**, 1717–1722 (1992).
- Braakman, I., Helenius, J. & Helenius, A. Role of ATP and disulphide bonds during protein folding in the endoplasmic reticulum. *Nature* **356**, 260–262 (1992).
- Segal, M.S., Bye, J.M., Sambrook, J.F. & Gething, M.J. Disulfide bond formation during the folding of influenza virus hemagglutinin. *J. Cell Biol.* **118**, 227–244 (1992).
- Chen, W., Helenius, J., Braakman, I. & Helenius, A. Cotranslational folding and calnexin binding during glycoprotein synthesis. *Proc. Natl. Acad. Sci. USA* **92**, 6229–6233 (1995).
- Molinari, M. *et al.* Contrasting functions of calreticulin and calnexin in glycoprotein folding and ER quality control. *Mol. Cell* **13**, 125–135 (2004).
- Marquardt, T., Hebert, D.N. & Helenius, A. Post-translational folding of influenza hemagglutinin in isolated endoplasmic reticulum-derived microsomes. *J. Biol. Chem.* **268**, 19618–19625 (1993).
- Hebert, D.N., Foellmer, B. & Helenius, A. Calnexin and calreticulin promote folding, delay oligomerization and suppress degradation of influenza hemagglutinin in microsomes. *EMBO J.* **15**, 2961–2968 (1996).
- Daniels, R., Kurowski, B., Johnson, A.E. & Hebert, D.N. N-linked glycans direct the cotranslational folding pathway of influenza hemagglutinin. *Mol. Cell* **11**, 79–90 (2003).
- Hammond, C., Braakman, I. & Helenius, A. Role of N-linked oligosaccharide recognition, glucose trimming, and calnexin in glycoprotein folding and quality control. *Proc. Natl. Acad. Sci. USA* **91**, 913–917 (1994).
- Hebert, D.N., Zhang, J.X., Chen, W., Foellmer, B. & Helenius, A. The number and location of glycans on influenza hemagglutinin determine folding and association with calnexin and calreticulin. *J. Cell Biol.* **139**, 613–623 (1997).
- Oliver, J.D., Roderick, H.L., Llewellyn, D.H. & High, S. ERp57 functions as a subunit of specific complexes formed with the ER lectins calreticulin and calnexin. *Mol. Biol. Cell* **10**, 2573–2582 (1999).
- Tatu, U., Hammond, C. & Helenius, A. Folding and oligomerization of influenza hemagglutinin in the ER and the intermediate compartment. *EMBO J.* **14**, 1340–1348 (1995).
- Singh, I., Doms, R.W., Wagner, K.R. & Helenius, A. Intracellular transport of soluble and membrane-bound glycoproteins: folding, assembly and secretion of anchor-free influenza hemagglutinin. *EMBO J.* **9**, 631–639 (1990).
- Copeland, C.S., Doms, R.W., Bolzau, E.M., Webster, R.G. & Helenius, A. Assembly of influenza hemagglutinin trimers and its role in intracellular transport. *J. Cell Biol.* **103**, 1179–1191 (1986).
- Tatu, U., Braakman, I. & Helenius, A. Membrane glycoprotein folding, oligomerization and intracellular transport: effects of dithiothreitol in living cells. *EMBO J.* **12**, 2151–2157 (1993).
- Ray, M.K., Yang, J., Sundaram, S. & Stanley, P. A novel glycosylation phenotype expressed by Lec23, a Chinese hamster ovary mutant deficient in α -glucosidase I. *J. Biol. Chem.* **266**, 22818–22825 (1991).
- Wilson, I.A., Skehel, J.J. & Wiley, D.C. Structure of the haemagglutinin membrane glycoprotein of influenza virus at 3 Å resolution. *Nature* **289**, 366–373 (1981).
- Chen, W. & Helenius, A. Role of ribosome and translocon complex during folding of influenza hemagglutinin in the endoplasmic reticulum of living cells. *Mol. Biol. Cell* **11**, 765–772 (2000).
- Peterson, J.R. & Helenius, A. In vitro reconstitution of calreticulin-substrate interactions. *J. Cell Sci.* **112**, 2775–2784 (1999).
- Air, G.M. Sequence relationships among the hemagglutinin genes of 12 subtypes of influenza A virus. *Proc. Natl. Acad. Sci. USA* **78**, 7639–7643 (1981).
- Naeye, C.W. & Webster, R.G. Sequence of the hemagglutinin gene from influenza virus A/Seal/Mass/1/80. *Virology* **129**, 298–308 (1983).
- Mathieu, M.E., Grigera, P.R., Helenius, A. & Wagner, R.R. Folding, unfolding, and refolding of the vesicular stomatitis virus glycoprotein. *Biochemistry* **35**, 4084–4093 (1996).
- Wada, I., Kai, M., Imai, S., Sakane, F. & Kanoh, H. Promotion of transferrin folding by cyclic interactions with calnexin and calreticulin. *EMBO J.* **16**, 5420–5432 (1997).
- Fuerst, T.R., Niles, E.G., Studier, F.W. & Moss, B. Eukaryotic transient-expression system based on recombinant vaccinia virus that synthesizes bacteriophage T7 RNA polymerase. *Proc. Natl. Acad. Sci. USA* **83**, 8122–8126 (1986).
- Zagouras, P. & Rose, J.K. Carboxy-terminal SEKDEL sequences retard but do not retain two secretory proteins in the endoplasmic reticulum. *J. Cell Biol.* **109**, 2633–2640 (1989).
- Privalsky, M.L. & Penhoet, E.E. Influenza virus proteins: identity, synthesis, and modification analyzed by two-dimensional gel electrophoresis. *Proc. Natl. Acad. Sci. USA* **75**, 3625–3629 (1978).
- Kistner, O., Muller, K. & Scholtissek, C. Differential phosphorylation of the nucleoprotein of influenza A viruses. *J. Gen. Virol.* **70**, 2421–2431 (1989).
- Bullido, R., Gomez-Puertas, P., Albo, C. & Portela, A. Several protein regions contribute to determine the nuclear and cytoplasmic localization of the influenza A virus nucleoprotein. *J. Gen. Virol.* **81**, 135–142 (2000).
- Daniels, R.S., Douglas, A.R., Skehel, J.J. & Wiley, D.C. Analyses of the antigenicity of influenza haemagglutinin at the pH optimum for virus-mediated membrane fusion. *J. Gen. Virol.* **64**, 1657–1662 (1983).
- Daniels, R.S. *et al.* Antigenic analyses of influenza virus haemagglutinins with different receptor-binding specificities. *Virology* **138**, 174–177 (1984).
- Benham, A.M. *et al.* The CXXCXXC motif determines the folding, structure and stability of human Ero1-L α . *EMBO J.* **19**, 4493–4502 (2000).